Annals of Biomedical Engineering, Vol. 31, pp. 1132–1140, 2003
Printed in the USA. All rights reserved.

0090-6964/2003/31(9)/1132/9/$20.00

Initial Burst Measures of Release Kinetics from Fiber Matrices

ABRAHAM SAGIV,[1] NADIA PARKER,[2] VEENA PARKHI,[2] and KEVIN D. NELSON[2]

[1]WRI–Rabin Desalination Laboratory, Department of Chemical Engineering, Technion–Israel Institute of Technology, Haifa 32000, Israel and [2]Joint Program in Biomedical Engineering, The University of Texas at Arlington and The University of Texas Southwestern Medical Center at Dallas, Dallas, TX

(Received 8 April 2003; accepted 9 June 2003)

Abstract—A comprehensive axisymmetric diffusion model of drug release from a fiber is developed to account for both the initial burst (IB) phenomenon as well as the later diffusion-dominated release. This model is an enhancement over previous models in that a set of four IB parameters are calculated, which both describe the initial burst phenomenon as well as improve the fit for the diffusion-dominated release phase. This model is also an enhancement over previous models in allowing: finite dissolution volumes, finite stirring levels of the medium, and user-specified initial drug dispersion within the device. Five different drug release data sets are used to verify the model and to derive values for the IB parameters. Two of the data sets are from experiments conducted in this study, and the other three sets are from previously published data. These data sets were selected to cover a wide range of possibilities, i.e., from nearly 0% to nearly 100% of the total drug release during IB, yet the model handles all cases equally well. © *2003 Biomedical Engineering Society.* [DOI: 10.1114/1.1603753]

Keywords—Initial burst, Diffusion-controlled release, Fibers, Finite volume, Stirring.

INTRODUCTION

Drug release from a biodegradable polymer is classically considered to involve the following five simultaneous and sequential processes:[15,17] (1) water diffusion into the polymer, (2) polymer swelling, (3) drug dissolution, (4) drug diffusion out of the polymer, and (5) polymer dissolution. However, in reality what is typically observed is an initial burst (IB) release that happens at time points much too early and with much higher intensity than could possibly be expected to occur by the above sequence of events. In addition, as there are classical differential equations that describe diffusion (discussed in detail below), when one calculates this diffusion-controlled release, the IB points fall very far from expected values, even though the remainder of the data is well described by the theory. Therefore, based on these facts we postulate that the above list should have as its first event an initial burst release that is not governed by diffusion. The IB release is, however, then typically followed by diffusion-controlled release as would be expected from the above sequence of events and as is well described by the theory.[1,2,4,5,7,19,21]

Our approach then is to divide the total release, and therefore, the data set, into two subsets; the first subset is called the initial burst, and consists of those data points whose release rate is much greater than that observed in the remainder of the data.

The second subset consists of the rest of the points whose release kinetics are well described by classical diffusion theory; this subset of points is referred to as CDT. We then perform a curve fit using the CDT points from our experimental data to a diffusion-based mathematical model for release from a cylindrical device. This curve fit has a number of adjustable parameters that involve the IB release phase. Thus, this curve fit procedure provides a quantifiable value for the parameters to accurately and uniquely describe the IB release phase, as well as a very good fit of the CDT data. The uniqueness of the derived IB parameters will be determined mainly by the closeness of the present model to the exact solution.

In order to simplify our model, we restrict the analysis to cases in which the polymer swelling or erosion is negligible during the release time. That is to say, we assume changes in the matrix size or mechanical properties yield negligible effects on the release profiles over the time of interest. This restriction allows us to assume that the diffusion coefficient and device radius are constants over the period of release.

While it is not the purpose of this paper to postulate on the cause or mechanisms responsible for the IB phenomenon, there are some ''rules of thumb'' or possible explanations given in the literature, which help to understand the derived IB parameters of a given data set. It is known that the composition of the release devices affects both the IB and the diffusion release profiles. For example, the type and the amount of plasticizers and polymers control the drug diffusivity and the resulting release kinetics profiles.[14,22] One explanation of the IB phenom-

Address correspondence to A. Sagiv, 51 Homa U'Migdal st. K. Haim, Haifa 26268, Israel. Electronic mail: asagiv@netvision.net.il

enon is that the drug in a dry matrix is usually dispersed uniformly in the matrix creating an amorphous structure with high release rates. As the dissolution solution diffuses into the matrix, the amorphous structure turns gradually into a semicrystalline structure, resulting in solution-filled pores through which the drug continues to diffuse out, but at a slower rate.[6,8–10]

Another possible explanation is the presence of hydrophilic polymers or macromolecules in the matrix with hydrophilic drugs tends to increase the IB of the drug,[7] whereas a more hydrophobic polymer matrix tends to retard the drug release and reduces the IB phase.[3,6] One way to reduce the IB is by polymeric coating.[1,2,20] However, the coating's function depends on variations of its production conditions,[21] which create additional nonreproducible factors in the release profile. Therefore, cheaper methods are used to reduce the IB, such as additives to the drug–polymer matrix.[4,19] Significant IB reduction is achieved by modifying the drug amount and production conditions to achieve small particle size with a narrow size distribution.[5]

To verify our model, we fabricated two drug-delivery devices and obtained three sets of data from previously published studies. Our criterion for selecting data sets to analyze was based on various combinations of hydrophobic/hydrophilic drugs and polymers, including a polymer-coated device. The devices we fabricated in our laboratory are drug-loaded wet-spun fibers. One fiber contains a hydrophilic protein, bovine serum albumin (BSA) as the mock drug; the other contains a hydrophobic drug, aldose reductase inhibitor (ARI AL-3152, generously donated by Alcon Laboratories, Ft. Worth, TX). Both fibers are made of a hydrophobic polymer, poly(L-lactic acid) (PLLA). One of the published data sets comes from a melt suspension technique used to fabricate a cylindrical matrix based on the combination of a hydrophobic polymer and starch derivatives.[21] Bonding agents may significantly reduce the initial drug release rate.[19]

The present study is designed to provide IB parameters through a fit procedure of a new mathematical model developed in this study, to a specific release data set. These IB parameters may be used as a control tool for pharmacologists, physicians, and producers, to meet specific therapeutic requirements. An approximate analytical model, based on the diffusion release mechanism, is developed for a cylindrical, drug-loaded polymer matrix, independent of fabrication technique. The term ''approximate analytical model'' is discussed in detail in Ref. 13 for the diffusion through a slab. The solution of the diffusion equations is exact, except the initial condition. It is approximately satisfied using the residual approximation method.[12]

THEORY

We apply the approximate analytical method to fibrous geometry to account for the diffusion-controlled release. This method is verified for finite solution volumes, finite stirring intensities, and arbitrary initial load profiles.[13] This method is attractive since it is achievable by a simple iteration method. It is as accurate as other numerical methods,[18,20] and its accuracy is either identical or of the same level as existing exact solutions (Table 1 in Ref. 13).

We restrict the analysis to release processes in which two successive release mechanisms, IB and the CDT, are present. The diffusion-controlled profile is identified as those data points that lie on the curve calculated by the diffusion model. The IB profile is defined as those initial data points that do not fit the diffusion-controlled profile and have higher release rates. These IB data points must receive separate theoretical considerations, which are beyond the scope of the present study. The following underlying assumptions of the model are based on diffusion-controlled release mechanism.

(i) The diffusion coefficient, D, within the matrix is constant.
(ii) The rate of the drug release is slower than the rate of the solvent's wetting front.
(iii) There are negligible changes in matrix dimensions.
(iv) Fibers whose $(L/d)^2 \gg 1$, say $L/d \geqslant 5$, and cylindrical tablets, whose $L/d < 5$ and capped on both ends (i.e., axial diffusion is neglected) are valid cases of the present model.

The dimensionless Fickian diffusion equation of the drug release out of a cylindrical matrix is

$$\frac{\partial C}{\partial t} = \frac{\partial^2 C}{\partial r^2} + \frac{1}{r}\frac{\partial C}{\partial r}, \tag{1}$$

where the drug concentration, C', in the fiber is normalized by a characteristic concentration, C_0, $C = C'/C_0$; the radius coordinate, r', is normalized by the fiber radius; R; $r = r'/R$; and the time, t', is normalized by $t = t'D/R^2$.

The concentration function that satisfies Eq. (1) is

$$C(r,t) = C_\infty + \sum_{n=0}^{\infty} a_n J_0(\lambda_n r)\exp(-\lambda_n^2 t), \tag{2}$$

where J_0 is the first kind Bessel function of order zero.

Because of the symmetric conditions in the fiber and in the solution medium surrounding the fiber, the boundary condition at $r = 0$ is

$$\frac{\partial C(0,t)}{\partial r}=0. \tag{3}$$

The flux at $r=1$ is assumed to behave according to

$$\frac{\partial C(1,t)}{\partial r}=S[kC_b(t)-C(1,t)], \tag{4}$$

where the Sherwood number $S=hR/D$, h is the mass transfer coefficient on the fiber surface, k is the partition coefficient of the drug, and C_b is the drug concentration in the dissolution medium.

If the characteristic concentration, C_0, is taken as the initial average concentration in the fiber, then the drug balance in the fiber and in the dissolution medium yields

$$2\int_0^1 C(r,t)rdr+k\delta[C_b(t)-C_{b0}]=1, \tag{5}$$

where C_{b0} is the initial drug concentration in the dissolution medium, $\delta=v/\pi kR^2L$, and v is the medium volume.

The stationary concentration in the matrix, C_∞, is derived from Eq. (5), and the following stationary conditions are

$$C(r,\infty)=C_\infty=kC_b(\infty), \tag{6}$$

$$C_\infty=1-k\delta[C_b(\infty)-C_{b0}]. \tag{7}$$

The drug concentration in the medium, $C_b(t)$, is derived from Eqs. (2), (5), and (7):

$$kC_b(t)=C_\infty-\frac{2}{\delta}\sum_{n=0}^{\infty}\frac{a_n}{\lambda_n}J_1(\lambda_n)\exp(-t\lambda_n^2), \tag{8}$$

where J_1 is the first kind Bessel function of order 1.

The coefficients vector a_n should satisfy the initial condition in the medium, $C_b(0)=C_{b0}$. Together with Eq. (8) we have a check condition for a_n:

$$kC_{b0}=C_\infty-\frac{2}{\delta}\sum_{n=0}^{\infty}\frac{a_n}{\lambda_n}J_1(\lambda_n). \tag{9}$$

The vector λ_n is calculated from the following Eq. (10) derived from Eqs. (2), (4), and (8):

$$\frac{J_0(\lambda_n)}{J_1(\lambda_n)}=\frac{\lambda_n^2\delta-2S}{\delta S\lambda_n}. \tag{10}$$

The vector a_n in Eq. (2) is calculated from the initial condition

$$C(r,0)=f(r), \tag{11}$$

where $f(r)$ is a given arbitrary axis-symmetric profile of the initial drug load in the fiber.

Substitution of Eq. (11) into Eq. (2) yields

$$\sum_{n=0}^{\infty}a_nJ_0(\lambda_nr)=f(r)-C_\infty. \tag{12}$$

According to the weight residual method,[12] the vector a_n is approximated by multiplying Eq. (12) by $J_0(\lambda_m r)$ as the weight function and integration of Eq. (12) over the fiber cross section. These steps yield explicit equations for the coefficients a_n:

$$a_n=A_{nm}^{-1}\alpha_m, \tag{13}$$

where

$$A_{nm}=\int_0^1 J_0(r\lambda_n)J_0(r\lambda_m)rdr,$$

$$\alpha_m=\int_0^1 (f(r)-C_\infty)J_0(r\lambda_m)rdr.$$

The integers $m,n=0,1,...,N$. Usually, the results are accurate enough for $N=6-20$. The number N is determined by satisfying the check condition, Eq. (9), within three significant digits.

It is convenient to present drug release data in the form of fractional cumulative release F versus release time t. Accordingly, the cumulative drug release concentration function $Cb(t)$ in Eq. (8), together with Eqs. (7), (10), and (13), yield the following fractional release equation used to compare the present theory with the data:

$$F(t)=1-\frac{2}{C_\infty\delta}\sum_{n=0}^{\infty}\frac{a_n}{\lambda_n}J_1(\lambda_n)\exp(-t\lambda_n^2). \tag{14}$$

The model, Eq. (14), is analytically derived except the evaluation of the coefficients a_n in Eq. (13), which approximately satisfy the initial condition, Eq. (11). The diffusivity D and the mass transfer coefficient h of Eqs. (2)–(14) must either be known or adjusted to minimize the following expression, Eq. (15), using a simple iteration procedure:

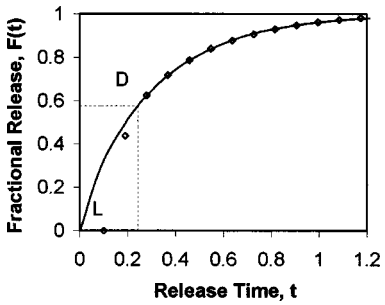

FIGURE 1. Fractional-release profiles. The diamonds are the Nadia 3.3–50 data set, described in the experimental section. The BSA is released from PLLA (200 kD) fibers, into a phosphate buffered saline. The solid line is calculated by Eqs. (14)–(16), with $t_L=0.101$, $D=9.244\times10^{-13}$ cm^2/s, $S=3$, and $k=1$.

$$\sum_{i=1}^{N1} |F(te_i)-Fe_i|\rightarrow\min, \tag{15}$$

where $N1$ is the number of the data points and Fe_i is the measured fractional amount released at time t_{ci}. Other parameters of the model are measurable and should be given.

Once the parameters D and h are determined, Eq. (14) is ready to describe the diffusion-controlled segment of the release kinetics. Therefore, initial data points that deviate from the diffusion curve should belong to the IB dataset. Figure 1 describes the two release types. The first two points and the point D describe the IB curve. For $t\geqslant t_D$, in Fig. 1, the drug release is diffusion controlled. The point L is the initial measured release time, while t_L is the lost release time because of the IB existence. If there is an IB, then the t_L becomes an additional adjustable parameter in the iteration procedure. Since t_L is the time interval between the initial point of the extrapolated diffusion curve and the real initial release time, point L (Fig. 1).

In the absence of an IB theory, the IB data points are extrapolated up to the intercept point with the diffusion curve for approximate determination of the point D (Fig. 1). Given the points D and L, the IB parameters may be defined as follows:

(1) IB duration, $t_{\rm IB}=t_D-t_L$.
(2) Amount released by the IB stage, $F(t_D)$.
(3) Average IB release rate, $R_a=F(t_D)/t_{\rm IB}$.
(4) Equivalent diffusion release rate, $R_d=dF(ta)/dt$, where $ta=(t_D+t_L)/2$.
(5) Release rates ratio, IBI$\equiv R_a/R_d$, indicates the IB intensity, or, how fast the release happened in the IB section relative to the equivalent release by the diffusion-controlled mechanism.
(6) The IB profile. In the present study, it will be presented graphically by the experimental data, such as the first two points and the point D in Fig. 1.

Of the six IB parameters, the independent parameters are t_L, t_D, $F(t_D)$, and the IB profile.

All the measured release times t_e are shifted by t_L to fit the equivalent diffusion-controlled release times t as if there is no IB process to obtain zero release at zero time. Accordingly, the diffusion time:

$$t_i=t_{ei}+t_L, \tag{16}$$

where $i=1,2,...,N1$ experimental data points. The IB measure t_L is adjusted for the best fit of Eq. (14) to the diffusion-controlled release data set, as illustrated in Fig. 1, for $t\geqslant t_D$.

THEORY IMPLEMENTATION

The following procedure is used to adjust unknown parameters of the model and optimize the fit of $F(t)$, Eq. (14), to a given data set. The fit procedure excludes initial data points that exhibit steeper release rates than the rates of the later points. The results may be refined by additional fit procedure with further excluding or including initial data points that are close to or lie on the diffusion curve.

(1) Given: R, L, v, N, $f(r)$, $N1$ data points: Me_i, Me_∞, te_i', $i=1-N1$. Assume $k=1$, $S=3$.
(2) Calculate: $\delta=v/\pi kR^2L$; $\lambda_n\,(n=0-N)$ by Eq. (10); C_∞ by Eq. (7).
(3) Guess D, t_L.
(4) Convert data into a dimensionless form: $Fe_i=Me_i/Me_\infty$, $te_i=te_i'D/R^2+t_L\,(i=1-N1)$.
(5) Calculate $a_n\,(n=0-N)$, Eq. (13).
(6) Calculate $F(te_i)$, Eq. (14).
(7) For a first iteration, calculate

$$E1=\sum_{i=e}^{N1} |F(te_i)-Fe_i|,$$

where the first $e-1$ data points are excluded from the calculations of $E1$, as they fall in the IB range.
(8) For other iterations, calculate

$$E=\sum_{i=e}^{N1} |F(te_i)-Fe_i|.$$

(9) If $E\leqslant E1$, then $E1=E$, $D1=D$, $tl=t_L$.
(10) Repeat steps (3)–(9) until $|1-E/E1|<0.01$.
(11) Equation (14) is ready for implementation, such as computing the theoretical curve $F(te_i)$ for extrapolation purposes of the experimental data points, $Fe_i(te_i)$, $i=1-N1$.

MATERIALS AND METHODS

The following methods are a part of a patent-pending process, and experiments are used to provide data for Figs. 1 and 5, as part of the model verification and the IB parameter determination.

PLLA solution of 10 wt/v % is prepared by dissolving 1.0 g of PLLA (MW: 200,000) (Poly Sciences) in 10.0 ml of chloroform (Sigma Aldrich) and allowed to stir for 3 h to assure complete dissolution. Aldose reductase inhibitor (AL-3152, Alcon Laboratories, Fort Worth, TX) solution is prepared by the following procedure. A stock solution of 28 ml is prepared using a 75:25 ratio of deionized water: isopropyl alcohol (IPA) (EM Science), 0.6013 ($\pm$0.0001) g of sodium bicarbonate, and 0.9116 ($\pm$0.0001) g of polyvinyl alcohol (PVA) are then added. Twenty ml of this stock solution was used to dissolve 4.00 g of ARI, thus giving a concentration of 20 wt/v % of ARI in the solution. This concentration (of 0.2 g/ml) is diluted with the excess starting stock solution to obtain a final concentration of 0.10 g/ml.

1.0 ml of this ARI solution is added to 10.0 ml of the PLLA solution and emulsified using a Vortex genie. This polymer emulsion is loaded into a 5 ml glass syringe and placed onto a syringe pump (Harvard Apparatus) and connected to a 21 gauge-dispensing needle (0.508 mm ID) via TYGON tubing.

The dispensing needle is submerged in isopropyl alcohol as the coagulating bath. The emulsion is extruded at a flow rate of 0.1 ml/min. The fiber is drawn from the coagulation bath at a rate of 5.92 m/min, giving a draw ratio of 10.7 (winding linear velocity to mean linear extrusion velocity). The diameters for these fibers are 50 ± 10 μm, and are called Nadia 3.3–50.

Four fibers, 4.0 in. (10.16 cm) in length are individually submerged in 1.0 ml of phosphate buffered saline and incubated at 37 °C. At predetermined time points, the fluid is removed and replaced with an equal amount of fresh media. The withdrawn media is analyzed by HPLC using the following conditions. The column is a Sephasil Protein column (No. 9642024, Pharmacia Biotech 250 $\times$4.6 mm) and the mobile phase consists of 30:70 acetonitrile (Sigma Aldrich): pure water with 3.5 g of sodium phosphate monobasic (0.5% of the volume of pure water) (NaH2PO4) (Fisher Scientific), and adjusted to pH 5.98 with sodium hydroxide (EM Science). The mobile phase flow rate is 2.0 ml/min. 100 μL of sample is injected and the UV absorbance is monitored at 220, 273, and 280 nm. ARI concentration is determined from a calibration curve.

The MWCal Veena 200/20 fibers were made of the same material as the Nadia's fibers (PLLA, 200kD). These fibers are loaded with bovine serum albumin (Sigma-Aldrich) as the mock drug. This is accomplished by dissolving the polymer in chloroform at a concentration of 1.0 g PLLA in 10.0 ml chloroform (Aldrich), then adding 400 μl of the aqueous phase, which is 50% w/w BSA in deionized water. A uniform emulsion is prepared by using a 10 cc glass syringe and an 18-gauge needle. The solution is drawn into and out of the syringe approximately 15–20 times to make the emulsion. This emulsion is extruded into isopropyl alcohol at a rate of 0.06 ml/min through a 21-gauge stainless steel needle (0.508 mm/ID) and wound at 5.9 m/min to produce a draw ratio of 20. These fibers are 56 μm in diameter and cut to 10.0 m lengths and incubated at 37 °C in 3.0 ml of phosphate buffered saline containing 0.01 wt % thimerosal as a broad-spectrum antibiotic. At regular intervals, the fluid is completely removed and replaced with fresh. The removed solution is analyzed using a Coomassie Brilliant Blue protein assay (Pierce, Rockford, Illinois) according to the manufacturer's recommended protocol. The concentration is determined from our calibration curve.

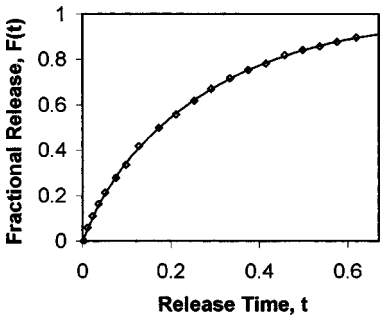

FIGURE 2. Fractional-release profiles. The diamonds are existing data of [Ref. 16, Fig. 1, empty circles]. The leavamisole is released from poly(ϵ-caprolactone) (147 kD) rods into a medium similar to that encountered in the rumen of cattle medium. The solid line is calculated by Eqs. (14)–(16), with $t_L=0.00315$, $D=1.222\times10^{-7}$ cm^2/s, $S=3$, and $k=1$.

RESULTS

In the absence of IB theories, the IB process is determined by excluding experimental initial data points that deviate from the diffusion curve. Such points are the first two points in Fig. 1. Consequently, the point L in Fig. 1 is precisely determined by applying Eqs. (14)–(16) to the experimental data points for $t \geqslant t_D$. The point D is approximated by the interception of the IB profile, which is a curve drawn through the experimental initial data points (for example, the first two points and the point D, of Fig. 1), with the diffusion curve of Eqs. (14)–(16) fit to the data points of $t \geqslant t_D$.

The release experiments conducted in this study yield data shown in Figs. 1 and 5. Other data of existing studies are shown in Figs. 2–4. Applying Eqs. (14)–(16) to the experimental data, yields the required IB parameters for the description of the IB phenomenon. In the

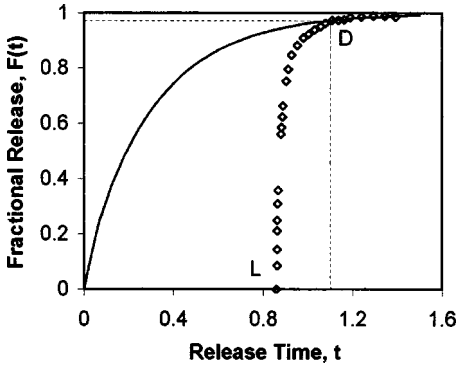

FIGURE 3. Fractional-release profiles. The squares are existing data of [Ref. 11, Fig. 6(c), millirods 1]. The trypan blue is released from PLGA rods into a PBS medium. The solid line is calculated by Eqs. (14)–(16), with $t_L = 0.859$, $D = 1.91 \times 10^{-9}$ cm^2/s, $S = 3$, and $k = 1$.

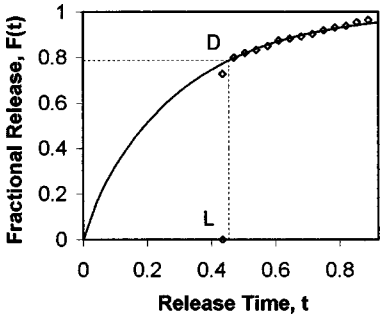

FIGURE 5. Fractional-release profiles. The diamonds are the MWCal Veena 200/20 data set, described in the experimental section. The BSA is released from PLLA (200 kD) fibers, into a phosphate buffered saline. The solid line is calculated by Eqs. (14)–(16), with $t_L = 0.435$, $D = 4.532 \times 10^{-13}$ cm^2/s, $S = 3$, and $k = 1$.

absences of information about the Sherwood number S, and the partition coefficient between the polymer and the dissolution medium, k, $S = 3$, and $k = 1$ were assumed for the fit procedure of Eqs. (14)–(16) to the release data shown in Figs. 1–5. Different values of S and k result in different IB values.

Bovine serum albumin release data from the Nadia 3.3–50 poly (L-lactic acid) [fibers, described in the experimental section, are shown in Fig. 1]. The fiber dimensions are 0.05 mm diam and 4.0 in. (101.6 mm) length. The fibers were immersed in 1.0 ml of phosphate buffered saline. The first two points and the point D, describe the IB profile, while for $t \geqslant t_D$, the data are correctly described by diffusion release calculation. The fit of Eq. (14), to the data, yields the IB parameters: $t_L = 0.101$, $t_D = 0.243$, and $F(t_D) = 0.576$. Other data used in the calculations are $D = 9.244 \times 10^{-13}$ cm^2/s, $S = 3$, and $k = 1$.

Existing fractional release data[16] (Fig. 1 of Ref. 16) of leavamisole hydrochloride from cylindrical poly(ϵ-caprolactone) (MW = 147,000 Da) and an iron powder matrices having the dimensions 25 mm diam and 105 mm length, are shown in Fig. 2. The drug was released to an *in vitro* medium similar to that encountered in the rumen of cattle.[16] The matrices were coated by bioresorbable polymers of 100 μm thickness,[16] which is within the diameter tolerance. This coating is assumed to have negligible change in the overall diffusion coefficient, and no change in geometric properties; however, it does appear that the presence of the coating has had a substantial reduction in the initial burst. The matrix was capped on both ends to allow release by longitudinal area only.[16] Applying Eqs. (14)–(16) to the data of,[16] yields the IB parameter, $t_L = 0.00315$. Graphically, the points L and D are invisible, as both t_L and t_D tend to zero. Therefore, the assumption $F(t_D) \approx F(t_L) = 0.018$ gives a practical estimate of the amount released by the IB process, which is around 2% of the total drug released. Other data used in the calculations are $D = 1.222 \times 10^{-7}$ cm^2/s, $S = 3$, and $k = 1$.

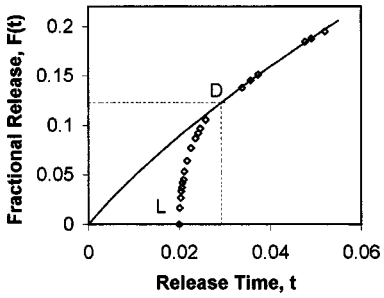

FIGURE 4. Fractional-release profiles. The diamonds are existing data of [Ref. 10, Fig. 2(B), TES]. The testosterone is released from PLLA rods into a dichloromethane medium. The solid line is calculated by Eqs. (14)–(16), with $t_L = 0.02$, $D = 4.04 \times 10^{-10}$ cm^2/s, $S = 3$, and $k = 1$.

Existing release data [Ref. 11, Fig. 6(c), millirod 1] of a trypan blue dye from a poly(D,L-lactic-co-glycolic acid) (PLGA) matrix in 10 ml phosphate buffered saline (PBS), are shown in Fig. 3. The cylindrical millirod dimensions are 1.6 mm diam and 10 mm length. Equations (14)–(16) are applied to these data yielding the following IB parameters: $t_L = 0.859$, $t_D = 1.106$, and $F(t_D) = 0.973$. Other data used in the calculations are $D = 1.91 \times 10^{-9}$ cm^2/s, $S = 3$, and $k = 1$.

Existing testosterone release data of [Ref. 10, Fig. 2(B), TES] from poly(L-lactic acid) [rods containing 10% of the drug, are shown in Fig. 4. The rod dimensions are 1 mm diam and 10 mm length. The drug was released into 5 ml of phosphate buffer adjusted isotonically with sodium chloride. Equations (14)–(16) are applied to the data of[10] yielding the following IB parameters: $t_L = 0.02$, $t_D = 0.0292$, and $F(t_D) = 0.123$. Other data used in the calculations are $D = 4.04 \times 10^{-10}$ cm^2/s, $S = 3$, and $k = 1$.

TABLE 1. IB parameters of the data in Figs. 1–5, arranged in an ascending order of t_L.

Fig. No.	t_D	t_L	T_L[f] (Days)	$T_D - T_L$ (Days)[g]	$F(t_D)$	Ra[c]	Rd[d]	IBI[e]
2	NA[a]	0.00315	0.470	NA[a]	~0.0180[b]	NA[a]	5.50	NA[a]
4	0.0292	0.0200	1.40	0.660	0.123	13.4	3.67	3.60
1	0.243	0.101	7.90	11.0	0.576	4.05	1.74	2.30
5	0.454	0.435	87.0	3.80	0.787	41.4	0.709	58.0
3	1.10	0.859	33.0	9.30	0.973	4.04	0.127	32.0

[a] t_D cannot be derived from the data of Ref. 21.
[b] $F(t_D) - F(t_L)$, as $t_L \to 0$.
[c] $R_a = F(t_D)/(t_D - t_L)$.
[d] $R_d = FD((t_L + t_D)/2)$.
[e] IBI $= R_a / R_d$.
[f] T_L = dimensional t_L expressed in days.
[g] $T_D - T_L$ = dimensional IB duration in days.

Bovine serum albumin release data from the MWCal Veena 200/20 poly(L-lactic acid) (200 kD) fibers, described in the experimental section, are shown in Fig. 5. The fiber dimensions are 0.056 mm diam and 1000 mm length. The fibers were immersed in 3.0 ml of phosphate buffered saline. The application of Eqs. (14)–(16), to the data, yields the IB parameters: $t_L = 0.435$, $t_D = 0.454$, and $F(t_D) = 0.787$. Other data used in the calculations are $D = 4.532 \times 10^{-13}\,\mathrm{cm}^2/\mathrm{s}$, $S = 3$, and $k = 1$.

The IB parameters derived from Figs. 1–5 are listed in Table 1. Such a presentation is allowed, despite the arbitrarily selected data sets, because of the theoretical dimensionless release profile common to all data sets subject to the diffusion-controlled mechanism from fibrous devices. The values in Table 1 may easily be converted to dimensional values for practical purposes. For example, one may be interested in relating the effect of different production methods of the same biodegradable matrix material, to the IB parameters, or indicating dimensional values for a specific therapeutic treatment.

DISCUSSION

The assumptions set in the theoretical section enable the focus on two dominant and sequential release types: the IB release mechanism followed by the diffusion-controlled release mechanism.

The results in Figs. 1–5 and in Table 1 present a comprehensive description of the IB phenomenon. Existing release data as well as data resulting from release experiments described in the experimental section, cover a wide range of the IB phenomenon; from nearly zero IB to nearly the entire release during the IB phase. The two end IB points L and D (Fig. 1), bracket the measured IB profile. The application of Eqs. (14)–(16) to experimental data with $t \geqslant t_D$ yields the IB parameters for each data set. The excellent fit of Eqs. (14)–(16) to the data in Fig. 1 distinguishes clearly the first two IB data points from other points that lie on the diffusion curve. The fit also verifies Eq. (14) as the diffusion-controlled release model of a drug from fibers or end-capped cylinders, and determines the IB points, L and D, through which the IB parameters are derived.

Another example of the excellent fit of Eqs. (14)–(16) to the release data of Ref. 16 is shown in Fig. 2. In this example, $t_L \to 0$ ($t_L = 0.00315$), indicating that the release process is dominated entirely by diffusion-controlled phase. This result is expected since the cylindrical matrices are coated with bioresorbable polyesters.[16]

The other end of the IB versus diffusion-controlled release continuum is when the release profile is nearly entirely dominated by the IB process, as shown by the data of Ref. 11 in Fig. 3 [$F(t_D) = 0.973$].

In the present model, Eq. (14) is able to fit data with small as well as large amounts of drug released by IB processes, provided that there are initial data points that deviate from the diffusion curve.

Extremely high IB release rates are shown in Fig. 5, which dominates most of the release profile range [$F(t_D) = 0.787$].

Recall that the present analysis provides an exact solution, except the initial condition which is approximately satisfied. Accordingly, the closer $F(0)$ [Eq. (14)] to zero (in the case of $Cb_0 = 0$), the closer the present method to the exact solution. Calculations of $F(0)$ for the five data sets yield $F(0) = 1.178 \times 10^{-5} - 1.223 \times 10^{-5}$, which are pretty close to zero, $F(0) \approx 0$. Therefore, the present method and the exact solution yield practically same results which follows that the derived parameters are uniquely determined. However, there are two comments on this conclusion:

(1) The accuracy of t_D depends on the measurement accuracy of the data points in the IB phase. The nonlinear regression curve fit to the data points using

a standard least-squares method are applied to get the required extrapolation for the intercept point of t_D with the diffusion curve, Eq. (14).

(2) The curve fit procedure of Eq. (14) to the data is based on a standard least squares method.

Following these conclusions the accuracy level of the IB values depends entirely on the accuracy level of the data.

Table 1 illustrates the use of the IB parameters to select a proper drug delivery device. For example, one may select a matrix fabrication method out of several alternatives, which provides minimum t_L. Similar analysis may be applied to yield matrix selection based on other IB parameters, shown in Table 1.

Dimensionless presentation of the results in Table 1 enables arrangement of arbitrarily selected data sets, as well as related data sets, according to any IB measure. For example, IB parameters resulting from the release data sets of Figs. 1–5, are arranged, in Table 1, in an ascending order of t_L.

The main characteristic of the IB phenomenon is t_L, which indicates the lost therapeutic time because of the IB. The data sets in Table 1 present the fractional amount released range, $0.018 \leqslant F(t_D) \leqslant 0.973$, which is practically the entire possible range $[0 \leqslant F(t_D) \leqslant 1]$.

An interesting IB measure in Table 1 is the rates ratio, $1 \leqslant \mathrm{IBI} < \infty$, of the average IB release rate over the equivalent diffusion-controlled release rate. This measure indicates how high the IB release rate relative to the equivalent diffusion-controlled release rate (in the absence of the IB release). Therefore, the IBI is a measure of the IB intensity. As an example, the highest IBI of the data used in the present study, is shown in Fig. 5 and in Table 1. The average release rate R_a of the IB phase of the data in Fig. 5 is 58 times the equivalent diffusion-controlled release rate (IBI=58), while it is only 2.3 for the data in Fig. 1.

The IB profile between t_L and t_D needs a special theory related to the materials involved and fabrication methods. It is beyond the scope of the present study. In most cases the selection and design of the polymer matrix, fabrication conditions, coatings, etc., can be based on minimizing or maximizing IBI and t_L, based on therapeutic needs for any given drug delivery application.

The present analysis provides almost a complete description of the IB phenomenon through its parameters (the IB profile type parameters are not included in the present analysis). It provides methods for analytical evaluation of the parameters. The IB parameters offer the pharmacologists design and test tools for fabrication of drug delivery devices and means to evaluate the drug delivery profiles. Thereby, the present study contributes to the control release profiles to be close as much as possible, to the therapeutic profile.

CONCLUSIONS

The present approximate analytical model is verified for drug release from fibers or end-capped cylindrical devices, whether IB or diffusion controlled release are the dominant mechanisms.

Evaluating the present model with experimental data of both this study as well as other selected existing data yields a comprehensive description of the IB phenomenon.

Four independent IB parameters were identified and derived from the fitting procedure of the model to the data. These measures describe the IB section of the drug release process.

The IB parameters may be used as selection criteria for biodegradable fiber matrices for best meeting the therapeutic requirements regarding the drug release amount and rate.

One of the IB parameters, the IB profile, is determined by experimental data only. Therefore, a theory is needed for better control of the IB profile through its parameters.

ACKNOWLEDGMENT

The fiber fabrication in this study was supported by NIH Grant No. R01 NS 40592-01.

REFERENCES

[1] Chen, B. H., and D. J. Lee. Finite element analysis of slow drug release through deformed coating film: Effect of morphology and average thickness of coating film. *Int. J. Pharm.* 234:25–42, 2001.

[2] Chen, B. H., and D. J. Lee. Slow release of drug through deformed coating film: Effects of morphology and drug diffusivity in the coating film. *J. Pharm. Sci.* 90:1478–1496, 2001.

[3] Cook, T. J., G. L. Amidon, and V. C. Yang. Polypeptides for controlled release applications: Synthesis and preliminary characterization and release studies. *Int. J. Pharm.* 159:197–206, 1997.

[4] Ebube, N. K., A. H. Hikal, C. M. Wyandt, D. C. Don, L. G. Miller, and A. B. Jones. Sustained release of acetaminophen from heterogeneous matrix tablets: Influence of polymer ratio, polymer loading, and coactive on drug release. *Pharm. Dev. Technol.* 2:161–170, 1997.

[5] Geze, A., M. C. Venier-Julienne, D. Mathieu, R. Filmon, R. Phan-Luu, and J. P. Benoit. Development of 5-iodo-2′-deoxyuridine milling process to reduce initial burst release from PLGA microparticles. *Int. J. Pharm.* 178:257–268, 1999.

[6] Gopferich, A. Erosion of composite polymer matrices. *Biomaterials* 18:397–403, 1997.

[7] Ibim, S. M., A. A. Ambrosio, D. Larrier, H. R. Allcock, and C. T. Laurencin. Controlled macromolecule release from poly(phosphazene) matrixes. *J. Controlled Release* 40:31–39, 1996.

[8] Miyajima, M., A. Koshika, J. Okada, and M. Ikeda. Effect of

polymer/basic drug interactions on the two-stage diffusion-controlled release from a poly(L-lactic acid) matrix. *J. Controlled Release* 61:295–304, 1999.

[9] Miyajima, M., A. Koshika, J. Okada, A. Kusai, and M. Ikeda. Factors influencing the diffusion-controlled release of papaverine from poly(L-lactic acid) matrix. *J. Controlled Release* 56:85–94, 1998.

[10] Miyajima, M., A. Koshika, J. Okada, A. Kusai, and M. Ikeda. Mechanism of drug release from poly(L-lactic acid) matrix containing acidic or neutral drugs. *J. Controlled Release* 60:199–209, 1999.

[11] Qian, F., A. Szymanski, and J. Gao. Fabrication and characterization of controlled release poly(D,L-lactic-co-glycolide) millirods. *J. Biomed. Mater. Res.* 55:512–522, 2001.

[12] Reddy, J. N. An Introduction to the Finite Element Method. New York: McGraw-Hill, 1985, p. 46.

[13] Sagiv, A. Theoretical formulation of the diffusion through a slab—Theory validation. *J. Membr. Sci.* 199:125–134, 2002.

[14] Siepmann, J., F. Lecomte, and R. Bodmeier. Diffusion-controlled drug delivery systems: Calculation of the required composition to achieve desired profiles. *J. Controlled Release* 60:379–389, 1999.

[15] Streubel, A., J. Siepmann, N. A. Peppas, and R. Bodmeier. Bimodal drug release with multilayer matrix tablets: Transport mechanisms and device design. *J. Controlled Release* 69:455–468, 2000.

[16] Vandamme, T. F., and J. F. N. Mukendi. Controlled release of levamisole from poly-(ϵ-caprolactone) matrices. III. Effect of molecular weight and polymer coating on drug release. *J. Pharm. Sci.* 145:77–86, 1996.

[17] Vergnaud, J. M. Liquid transport processes in polymeric materials. Modeling and Industrial Applications. Englewood Cliffs, NJ: Prentice-Hall, 1991, Sec. 10-2.

[18] Vergenaud, J. M. Problems encountered for food safety with polymer packages: Chemical exchange, recycling. *Adv. Colloid Interface Sci.* 78:267, 1998.

[19] Vercruysse, C. W. J., E. A. P. De Maeyer, and R. M. H. Verbeeck. Fluoride release of polyacid-modified composite resins with and without bonding agents. *Dent. Mater.* 17:354–358, 2001.

[20] Wu, X. Y., and Y. Zhou. Finite element analysis of diffusional drug release from complex matrix systems. II. Factors influencing release kinetics. *J. Controlled Release* 51:57–71, 1998.

[21] Zhou, F., C. Vervaet, and J. P. Remon. Matrix pellets based on the combination of waxes, starches, and maltodextrins. *Int. J. Pharm.* 133:155–160, 1996.

[22] Zhou, Y., and X. Y. Wu. Finite element analysis of diffusional drug release from complex matrix systems. I. Complex geometries and composite structures. *J. Controlled Release* 49:277–288, 1997.